Pharm Res (2014) 31:1766–1778
DOI 10.1007/s11095-013-1281-3

RESEARCH PAPER

Thermodynamic and Kinetic Investigation on the Crucial Factors Affecting Adefovir Dipivoxil-Saccharin Cocrystallization

Kun Ma • Ying Zhang • Hongliang Kan • Linfeng Cheng • Ling Luo • Qing Su • Jing Gao • Yuan Gao • Jianjun Zhang

Received: 22 September 2013 / Accepted: 31 December 2013 / Published online: 13 February 2014

ABSTRACT

Purpose The aim of this study was to perform a thermodynamic and kinetic investigation on the crucial factors affecting the cocrystallization between adefovir dipivoxil (AD) and saccharin (SAC).

Methods Phase solubility diagrams and ternary phase diagrams were constructed based on the solubility data of AD, SAC and their cocrystals in ethanol, isopropanol and ethyl acetate at different temperatures. The conductimetric method was used to determine the induction time. A quantitative and intuitive technique modified from dissolution testing was employed to investigate the cocrystallization kinetics.

Results AD-SAC cocrystals exhibited different crystal habits but only one cocrystal polymorph was confirmed. The effects of several crucial factors, including the input amounts of two components, AD/SAC ratio, solvent and temperature, on the crystallization of single-component alone, cocrystal formation, cocrystal stability, supersaturation, nucleation, crystal growth and cocrystal yield were determined. Thermodynamic and kinetic parameters provided the rationale for this spontaneous cocrystallization system without the need of solvent evaporation and temperature change.

Conclusions This systemic investigation enriched the present understanding of thermodynamics and kinetics of cocrystals and built the groundwork for AD-SAC cocrystal scale-up.

K. Ma • Y. Zhang • H. Kan • L. Luo • Q. Su • J. Zhang (✉)
School of Pharmacy, China Pharmaceutical University
Nanjing 210009, China
e-mail: amicute@163.com

L. Cheng • J. Gao • Y. Gao
School of Traditional Chinese Medicine, China Pharmaceutical University
Nanjing 210009, China

K. Ma
Center for Drug Evaluation, State Food and Drug Administration
Beijing 100038, China

KEY WORDS adefovir dipivoxil · cocrystal · kinetics · nucleation · thermodynamics

ABBREVIATIONS

AD	Adefovir dipivoxil
API	Active pharmaceutical ingredient
CBZ	Carbamazepine
CCF	Cocrystal former
IND	Indomethacin
$K_{1:1}$	Complexation constant
K_{sp}	Solubility product
NCT	Nicotinamide
PSD	Phase solubility diagram
PTFE	Polytetrafluoroethylene
SAC	Saccharin
SEM	Scanning electron microscopy
TPD	Ternary phase diagram
XRPD	X-ray powder diffraction

INTRODUCTION

Cocrystallization has been an efficient non-covalent approach for the modification of some compounds without changing their chemical structure (1). By the formation of cocrystal, the solubility/dissolution (2), physical/chemical stability (3,4), mechanical properties (5), and bioavailability (6) can be enhanced. Generally, a combination of several enhancements can be simultaneously achieved (7). However, the preparation of cocrystal by solution-mediated phase transformation and its control face some difficulties due to the complex parameters involved in the cocrystallization process (8). The relationship between the equilibria among the three solid phases is complicated (9). There are also the potential partial cocrystallization and the undesired molecular interaction (10).

To achieve a robust cocrystallization process, it is prerequisite to identify the key factors affecting cocrystallization

between the active pharmaceutical ingredient (API) and its cocrystal former (CCF) in the solvent. Phase solubility diagrams and triangular phase diagrams are helpful for the phase composition of API-CCF-solvent combination, a three-component/four-phase system (8,11). These diagrams are dependent on the components and many experimental conditions (4,12). Each set of API-CCF-solvent at a given condition has the specialized phase diagrams. In the literatures, the thermodynamic parameters, such as solubility products (K_{sp}) and complexation constants (K_{11}), were generally obtained based on the assumption that the CCF concentration was far less than $K_{sp}K_{11}$, the product of K_{sp} and K_{11}. So far, no exception has been reported.

Kinetic study is essential for collecting information about the intermediate process of cocrystallization and identifying the optimal cocrystallization conditions. Few studies reported the cocrystallization kinetics. *In-situ* attenuated total reflectance (ATR)−FTIR spectroscopy has been used to monitor the kinetics of carbamazepine-nicotinamide-ethanol system during cooling cocrystallization (13). However, this facility is not readily available. Furthermore, it is hard to determine the real amount of cocrystal and has large deviations of the measured concentration (14). An *in-situ* video has also been used to monitor the crystallization process in the reactor (15). Solubility data and cocrystal amount were not available in this study as well. For a system containing denser solid in suspension, visual problem will occur. Different technique has its respective advantages and disadvantages. The combination of various techniques may be encouraged to achieve better efficiency and accuracy.

Previously, adefovir dipivoxil (AD)-saccharin (SAC) cocrystal was prepared using an *in-situ* precipitation method to simultaneously enhance the chemical stability and dissolution of AD, a bis(pivaloyloxymethyl) prodrug of the antiviral nucleotide analogue, adefovir (3,16). Also, different coformers resulted in different AD cocrystal which exhibited different physico-chemical performance (17). During the preparation of AD-SAC cocrystal, the general precipitation methods including solvent evaporation (7) and cooling (18), are not necessary. This makes AD-SAC a valuable and unique cocrystal system to study cocrystal.

For solution-mediated phase transformation, solvents play important roles and may responsible for the various characteristics of the formed crystals (19). In our previous study, only ethanol was used as the solvent to investigate the thermodynamics of AD-SAC cocrystal (20). Some key parameters for the formation of AD-SAC, the nucleation and growth of cocrystal are missed. Here, the cocrystallization between AD and SAC are further investigated to acquire the important thermodynamic/kinetic parameters. Moreover, the intermediate process of cocrystallization is also studied using a continuous and intuitive technique with good operability and applicability.

MATERIALS AND METHODS

Materials

AD (form I, 99.8% purity) was purchased from Saifule Pharmaceuticals Co., Ltd. (Leping, China). SAC (99.0% purity) was obtained from Sigma-Aldrich Inc. (Shanghai, China). Methanol of HPLC grade was purchased from E. Merck (Darmstadt, Germany). All other chemical reagents were purchased from Sinopharm Chemical Reagent Co., Ltd. (Shanghai, China).

Methods

Solubilities of AD and SAC in Three Solvents

The solubilities of AD in SAC solution, AD and SAC in pure solvents were measured in ethanol, isopropanol and ethyl acetate. The concentration ranges of SAC solution were 0.0120–0.1474 mol/L in ethanol, 0.0097–0.1092 mol/L in isopropanol and 0.0091–0.1769 mol/L in ethyl acetate, respectively. The glass vial containing excess solid and 2 ml of pure solvent or SAC solution was placed in a water bath and stirred with a magnetic bar. The water in this bath was circulated into and out from a low temperature bath (temperature range of −5 ~ 100°C, a precision of ±0.01°, Nanjing ShunMa Equipment Co., Ltd.) using two peristaltic pumps (BT100-2 J, Baoding Longer Precision Pump Co., Ltd.) at a flow rate of about 100 ml/min to keep the temperature constant. The temperatures studied were 4, 20, 30 and 40°C. After stirring for 3 h, which was preliminarily demonstrated to be enough for AD to reach the solubility equilibrium, the slurry was filtered with a 0.22 μm nylon filter (Millipore, Bedford, MA). The subsequent filtrate was appropriately diluted with methanol. Each experiment was repeated in triplicates. The AD concentration was determined by a Shimadzu 2010 AHT high performance liquid chromatogram system (Kyoto, Japan) as reported previously (3). The simultaneous determination of AD and SAC was carried out on a Shim-Pack VP-ODS column (4.6 mm*150 mm, 5 μm) which was kept at 30°C. Isocratic mobile phase was a mixture of methanol and 0.02 mol/L potassium dihydrogen phosphate (pH 6.0) (58:42 v/v) at a constant flow rate of 1.0 ml/min. The detector was set at 260 nm and the injected volume of sample solution was 20 μl (3).

Phase Solubility Diagrams and Ternary Phase Diagrams

Phase solubility diagrams were constructed to show the solution concentrations at equilibrium with solid phases and the relative thermodynamic stability of cocrystal. The solubility products (K_{sp}), complexation constants (K_{11}) between AD and SAC in the solution, and the standard free energy change

(ΔG°) were calculated based on the solubility data. Ternary phase diagrams of the AD-SAC-solvent systems at four different temperatures were also established to show the total composition of solid phases and liquid phases at equilibrium and the comparative region for effective cocrystallization.

For the AD-SAC cocrystal with a 1:1 stoichiometry (3), the equilibrium reactions in the four-phase system are given by (11,21,22)

$$AD{-}SAC_{solid} \overset{K_{SP}}{\longleftrightarrow} AD_{solution} + SAC_{solution} \tag{1}$$

$$AD_{solution} + SAC_{solution} \overset{K_{11}}{\longleftrightarrow} AD{-}SAC_{solution} \tag{2}$$

K_{11} can be given as

$$K_{11} = \frac{[AD{-}SAC]}{[AD][SAC]} = \frac{[AD{-}SAC]}{K_{sp}} \tag{3}$$

The cocrystal solubility can be expressed as (11),

$$[AD]_{total} = \frac{K_{sp}}{[SAC]_{total} - K_{11}K_{sp}} + K_{11}K_{sp} \tag{4}$$

According to Eq. (4), the values of K_{sp} and K_{11} in three solvents at a certain temperature were obtained by a nonlinear regression using SPSS 10.0 (SPSS, Chicago, IL, USA).

Kinetics of Nucleation and Crystal Growth

To quantitatively determine the nucleation and dynamic growth of AD-SAC cocrystal, a dissolution tester (ZRS-8G, TDTF technology Co., Ltd., China) was creatively used for this purpose. The formation kinetics of solid cocrystal as a function of solvent and supersaturation was studied at 20± 0.2°C (n=3).

AD and SAC solutions (0.05–0.20 mol/L) in three solvents were filtered through 0.22 μm membrane filters to avoid impurities which may activate the heterogeneous nucleation. 100 ml of preheated AD solution (20°C) and 100 ml of preheated SAC solution (20°C) prepared using the same solvent (ethanol, isopropanol or ethyl acetate) were mixed in one dissolution vessel (V≈250 ml). The distance between the bottom of the paddle blade and the bottom of the vessel was 15±1 mm. The rotation speed was set at 100 rpm to maintain a homogeneous crystallization process inside the vessel. The solvent evaporation was controlled by a vessel cover specially designed for this study. The mean solvent loss was determined to be 1.1% and 3.1% at 1 h and 3 h, respectively. The determination for most of the cocrystallization kinetics was completed in 30 min so the solvent evaporation in the vessels was negligible.

The induction period is defined as the time lag for a solution to reach supersaturation where an experimentally accessible quantity of new phase is detectable. Fluorescence (23), electronic microscopy (24), intensity of transmitted light (25), turbidity (26) and conductivity (27) have been reported for the determination of the induction period. In this study, the order of the appearance of nuclei and nucleation induction period was assessed by the conductimetric method which has been demonstrated to be reliable (28). The induction time was determined from recording the time evolution of the solution conductivity, which is verified to be unambiguously related to the amount of the precipitates (27). A conductivity meter (DDSJ-308F, Shanghai Precision & Scientific Instrument Co., Ltd.) with a measuring range of 0.000 μS/cm~199.9 mS/cm, a resolution of 0.001 μS/cm and a precision of±0.5% was employed. The distance between the bottom of the electrode and the bottom of the vessel was set at 20±1 mm. REXDC 2.0 software was used to record the conductivity data. The conductivity was plotted against time. The transition point with an obvious decline in conductivity curve was taken as the induction period. The good repeatability of the method was confirmed using AD/SAC (0.1:0.1 mol/L:mol/L) at 20°C. The RSD of solution conductivity before induction time was 0.96% and 1.23% in ethanol and ethyl acetate, respectively. The RSD of induction time was 6.27% and 8.73% in ethanol and ethyl acetate, respectively. For AD/SAC (0.05:0.07 mol/L:mol/L) in ethanol, the RSD of induction time was 5.66%.

Sampling was performed at intervals. After the solid on the pre-weighed polytetrafluoroethylene (PTFE) filter membrane (0.22 μm pore size) for suction filtration was transferred into a pre-weighed flat-base glass vial, all the membranes and vials were dried under vacuum at 25°C and accurately weighed after 2 h. It was verified that no weight change occurred to the filter membrane after the filtration of three pure solvent and the subsequent vacuum drying. The weight of obtained cocrystal at a given time was the sum of the weight gain of the dried vial and the filter membrane. Appropriate amount of cocrystal in the vial was dissolved and diluted in methanol to a certain concentration prior to HPLC analysis.

After the experiment, the cocrystal was collected by filtering the slurry in the vessels and vacuum dried at 25°C for 6 h prior to further characterization.

Polymorph and Crystal Habit of the Cocrystal in Three Solvents

XRPD patterns of the dried cocrystal were recorded using a Bruker D8 Advance powder diffractometer (Karlsruhe, Germany) with Cu-Kα radiation (1.5406 Å). The samples were gently consolidated in an aluminium holder and scanned

at 40 kV and 40 mA from 5 to 45° 2θ using a scanning speed of 2°/min and a step size of 0.02°.

The morphologies of the final products were examined under SEM (Hitachi S3400, Tokyo, Japan) at 20 kV. All samples were attached on a brass stub using carbon double-sided tape. Fractured samples were glued and mounted on metal sample plates. The samples were coated with gold using a sputter coater (Fison Instruments, UK) at 2.0 kV and 25 mA for 10 min.

RESULTS AND DISCUSSION

Crystal Form and Crystal Habit

For each cocrystal, its stoichiometry at different sampling time was determined by assaying AD and SAC using HPLC. The weight percentages of AD and SAC in the dried solid were determined to be 73.01–75.32% and 25.68–27.86%, respectively. This agrees well with the 1:1 stoichiometry of cocrystal, since the theoretical percentages of two components in AD-SAC cocrystal are 73.25% and 26.75%. This result demonstrates that the stoichiometry is constant at 1:1 since the cocrystal precipitation starts from the solution, regardless of the AD/SAC ratio and amount. As shown in Table I, in three solvents, both AD and SAC have much higher solubility in three solvents than the cocrystal. There is no change in the amount of solvent and temperature, so the crystallization of individual AD or SAC will hardly occur. In this respect, this cocrystallization appears to be more favored than the crystallization of single-component, over the solvent evaporation or cooling method, because in some cases the components in those systems will precipitate individually by decreasing the solvent amount or temperature, the two vital parameters for the solubility of the compounds.

The XRPD patterns of AD-SAC cocrystals prepared from ethanol, isopropanol and ethyl acetate are presented in Fig. 1 (only final products shown). The cocrystals formed in ethanol (Fig. 1a) and isopropanol (Fig. 1b) have the similar patterns. Cocrystal formed in ethyl acetate (Fig. 1c) has a new weak peak at 2θ of 9.38 and a weakened peak at 2θ of 18.66. The other diffraction peaks of b and c are similar. The XRPD results suggest the three cocrystals are most possibly the same polymorph. The XRPD of the samples at the first sampling point was similar to that of the final products, which indicates that the 1:1 cocrystal is formed simultaneously when the precipitation happened in the three organic solvents.

Figure 2 shows the SEM images of AD-SAC cocrystals from ethanol (Fig. 2a), isopropanol (Fig. 2b) and ethyl acetate (Fig. 2c). AD-SAC cocrystal produced in ethanol is plate-shaped, whereas the crystals obtained from ethyl acetate and isopropanol are needle-shaped. This has also been confirmed by observing the morphology of these cocrystals under a Leica DM LM/P microscope (Leica,Germany) (data not shown). The crystal habit change may affect their mechanical properties, which is worthy of further studies.

Phase Solubility Diagrams (PSDs)

The PSDs show the solubility of AD, SAC, and AD-SAC as a function of SAC concentration, expressed in molarity. PSDs are useful for studying the dependence of cocrystal formation on the solution composition and complexation. They are commonly used to evaluate the complexation constants of APIs and solubility product constants (29).

The previous thermodynamics study of AD-SAC cocrystal in ethanol has two drawbacks (20). First, the gas-bath thermostatic oscillator used for the conventional oscillation solubility test had a higher temperature fluctuation (± 4°C). Second, 72 h is needed to reach the solubility equilibrium. During this period, the degradation occurred to AD. Both of them could affect the accuracy of the measured solubility data and the calculated K_{sp} and K_{11} data. So in this work, we re-measured the solubility in ethanol with improved experimental setup which has precise temperature control and reduced required time (less than 3 h) to reach solubility equilibrium by introducing magnetic stirring. These improvements have been verified by the relatively small SD values of solubility data shown in Table I. Thus, the solubility, K_{sp} and K_{11} determined in this study is much more accurate.

AD solubility is dependent on SAC concentration, solvent type and temperature. It is clearly indicated that existence of SAC in solution decreases the solubility of AD in three solvents. This suggests the existence of distinct solution complexation. As shown in Fig. 3, the cocrystal solubility decreases nonlinearly with increasing SAC concentration in the solvents. The data fitted with non-linear regression equations are presented in Table II. The predicted curves are in very good agreement with ($R^2 > 0.99$) the experimental solubility values in three solvents.

As listed in Table II, K_{sp} and K_{11} are affected by temperature and solvent. K_{sp} is proportional to the solubility of cocrystal in each given solvent and increases significantly with increasing temperature in three solvents. At the same temperature, the order of magnitude *for* K_{sp} values is ethanol > isopropanol > ethyl acetate.

As an indicator of solution complexation, K_{11} decreases with increasing temperature, which is opposite to K_{sp}. At a given temperature, it is obvious that K_{11} is higher in ethyl acetate and isopropanol than that in ethanol. It was concluded that higher solubility of a single solute in the solvent is driven by their higher solute-solvent interactions, and lower solubility in a solvent would therefore favor the solute-solute interactions and facilitate the complex formation in the solvent (30,31). However, for cocrystallization system, the three solutes may have different or inverse affinity with the same solvent. It may be unsubstantial to evaluate the complexation in the four-phase

Table I Solubilities of AD, SAC and AD-SAC Cocrystal and the Thermodynamic Parameters in Three Solvents at Different Temperatures

Solvent	T/K	AD(mol/L)	SAC(mol/L)	AD-SAC(mol/L)	ΔG°(kJ/mol)
Ethanol	277	0.301 ± 0.0078	0.0893 ± 0.0025	0.0196 ± 0.0012	−13.9
	293	0.796 ± 0.0102	0.129 ± 0.0052	0.046 ± 0.0024	−12.1
	303	0.902 ± 0.0113	0.146 ± 0.0041	0.054 ± 0.0026	−12.1
	313	1.24 ± 0.013	0.167 ± 0.0036	0.102 ± 0.0032	−9.91
Isopropanol	277	0.265 ± 0.013	0.0672 ± 0.0014	0.0159 ± 0.0009	−13.8
	293	0.489 ± 0.014	0.086 ± 0.0032	0.0405 ± 0.0033	−12.8
	303	0.561 ± 0.017	0.105 ± 0.0019	0.0456 ± 0.0042	−12.7
	313	1.12 ± 0.012	0.143 ± 0.0023	0.0830 ± 0.0056	−10.2
Ethyl acetate	277	0.166 ± 0.0063	0.1334 ± 0.0031	0.0151 ± 0.0092	−14.4
	293	0.344 ± 0.0095	0.189 ± 0.0047	0.0516 ± 0.0038	−13.9
	303	0.382 ± 0.0024	0.211 ± 0.0053	0.0763 ± 0.0047	−13.6
	313	0.564 ± 0.0068	0.306 ± 0.0029	0.137 ± 0.0093	−10.4

system only according to the solubilities of components. For example, as shown in Table I, AD has the least solubility and SAC has the highest solubility in ethyl acetate (Table I). This makes it more complicated and difficult to assess the inter-solute interaction in a certain solvent using solubility data. In these situations, such as multi-components system, other thermodynamic parameters including K_{11} may serve well to evaluate the solute-solute interactions. The higher K_{11} at lower temperature in ethyl acetate and isopropanol indicates the stronger interaction between solutes AD and SAC which therefore leads to greater tendency for complex formation.

The carbamazepine-nicotinamide cocrystal (CBZ-NCT) (11) and the indomethacin-saccharin cocrystal (IND-SAC) (30) in organic solvents had the similar patterns of variation of K_{sp} and K_{11}. However, in the present study, K_{sp} values of AD-SAC are much smaller and the K_{11} values were much bigger

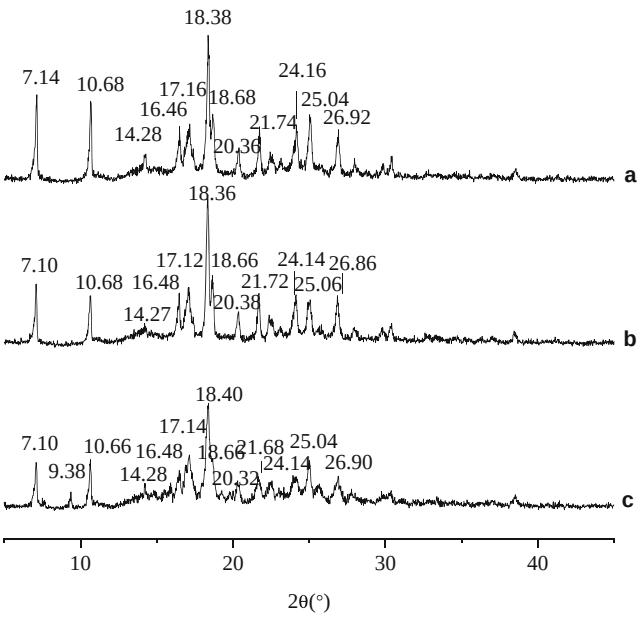

Fig. 1 XRPD patterns of AD-SAC cocrystal from ethanol (**a**), isopropanol (**b**), and ethyl acetate (**c**).

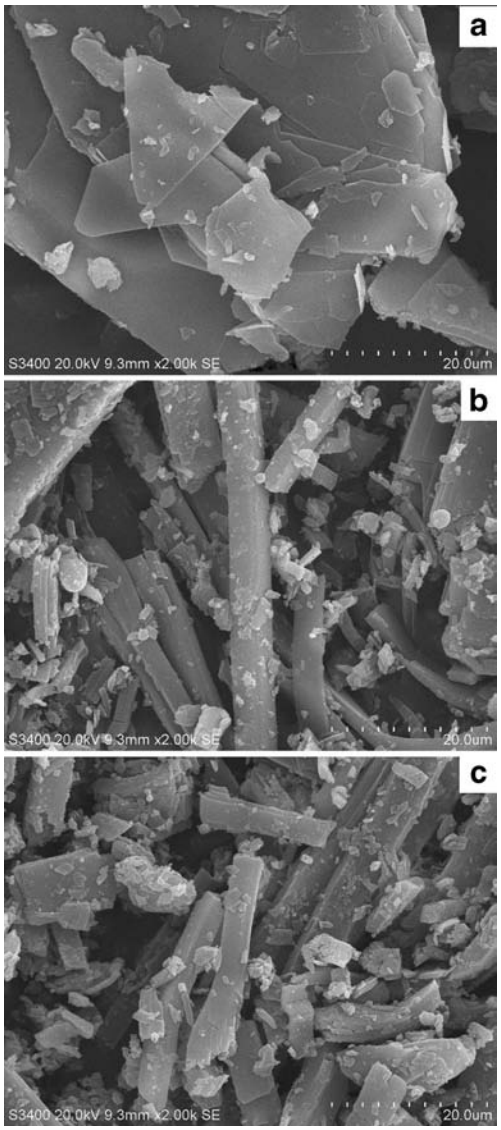

Fig. 2 The SEM pictures of AD-SAC cocrystals from ethanol (**a**), isopropanol (**b**), and ethyl acetate (**c**).

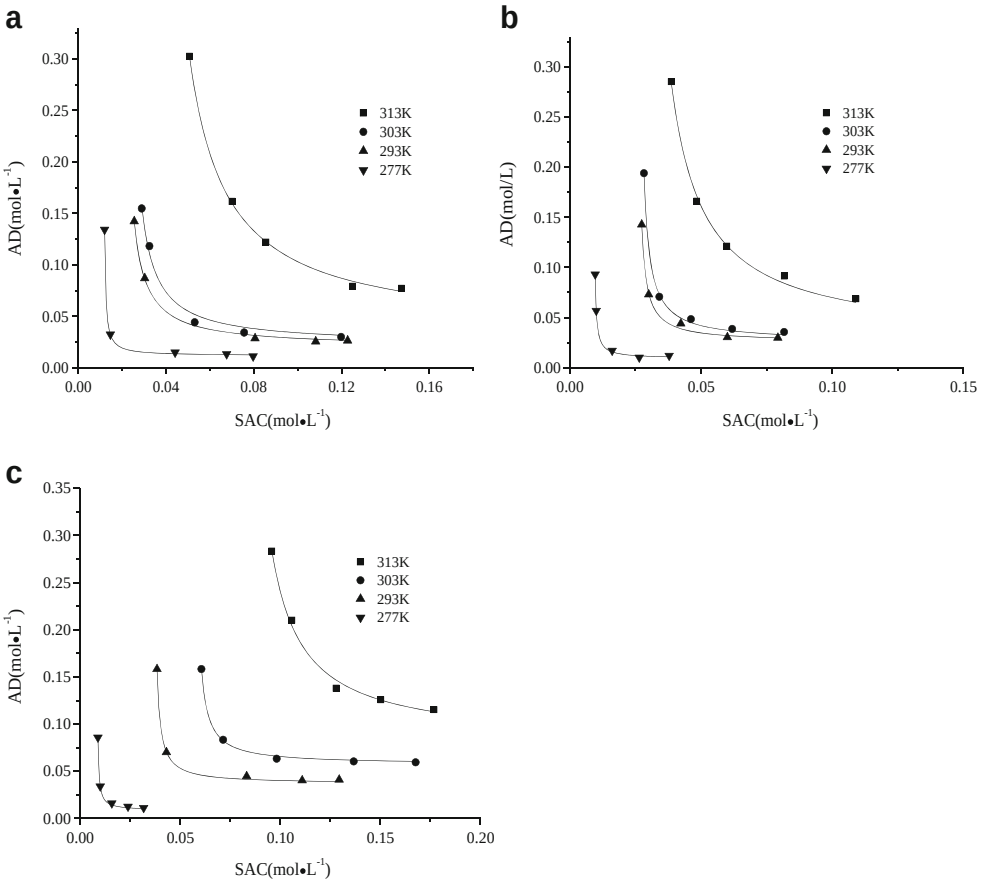

Fig. 3 Comparison of experimental and calculated cocrystal solubilities as a function of saccharin concentration in ethanol (**a**), isopropanol (**b**), and ethyl acetate (**c**) at different temperatures. Labeled points are measured values and *lines* are fitted values.

than CBZ-NCT and IND-SAC cocrystals. This implies that AD and SAC has higher interaction and make the formation of AD-SAC cocrystal easier. This is intuitively confirmed by the *in-situ* precipitation of AD-SAC without the need of solvent evaporation (3). To our knowledge, AD-SAC cocrystal is so far the only cocrystal that can be produced via *in-situ* precipitation without the necessity of solvent evaporation or cooling.

As listed in Table II, the product of K_{sp} and K_{11} in ethanol (0.0115–0.0335 mol/L) is very close to the SAC concentration studied (0.0120 to 0.1474 mol/L). It's similar in isopropanol or ethyl acetate. Thus, it is not suitable to neglect $K_{11}K_{sp}$ from the denominator in Eq. (4). If $K_{11}K_{sp}$ were neglected from the denominator when it was regarded as far less than the concentration of SAC, as reported by Nehm *et al.*(11) and

Table II Solubility Product Constant (K_{sp}) and Complexation Constant (K_{11}) of AD-SAC Cocrystal in Three Solvents at Different Temperatures Calculated by Non-Linear Regression Analysis

Solvents	T/K	Fitted curves	K_{sp}(mol^2/L^2)	K_{11}(L/mol)
Ethanol	277	$[AD]=6.51\times10^{-5}/([SAC]-1.15\times10^{-2})+1.15\times10^{-2}$ $R^2=0.999$	$(6.52\pm0.23)\times10^{-5}$	176.3 ± 2.10
	293	$[AD]=7.05\times10^{-4}/([SAC]-1.97\times10^{-2})+1.97\times10^{-2}$ $R^2=0.998$	$(7.05\pm0.17)\times10^{-4}$	27.99 ± 0.63
	303	$[AD]=1.10\times10^{-3}/([SAC]-2.08\times10^{-2})+2.08\times10^{-2}$ $R^2=0.993$	$(1.10\pm0.013)\times10^{-3}$	18.96 ± 0.37
	313	$[AD]=4.62\times10^{-3}/([SAC]-3.35\times10^{-2})+3.35\times10^{-2}$ $R^2=0.998$	$(4.62\pm0.13)\times10^{-3}$	7.27 ± 0.26
Isopropanol	277	$[AD]=4.56\times10^{-5}/([SAC]-9.17\times10^{-3})+9.17\times10^{-3}$ $R^2=0.998$	$(4.56\pm0.33)\times10^{-5}$	200.9 ± 1.49
	293	$[AD]=2.24\times10^{-4}/([SAC]-2.55\times10^{-2})+2.55\times10^{-2}$ $R^2=0.995$	$(2.24\pm0.22)\times10^{-4}$	114.3 ± 1.12
	303	$[AD]=3.83\times10^{-4}/([SAC]-2.60\times10^{-2})+2.60\times10^{-2}$ $R^2=0.998$	$(3.83\pm0.13)\times10^{-4}$	68.01 ± 0.51
	313	$[AD]=3.21\times10^{-3}/([SAC]-2.63\times10^{-2})+2.63\times10^{-2}$ $R^2=0.996$	$(3.21\pm0.22)\times10^{-3}$	8.18 ± 0.012
Ethyl acetate	277	$[AD]=4.32\times10^{-5}/([SAC]-8.54\times10^{-3})+8.54\times10^{-3}$ $R^2=0.998$	$(4.32\pm0.31)\times10^{-5}$	197.8 ± 1.61
	293	$[AD]=2.20\times10^{-4}/([SAC]-3.68\times10^{-2})+3.68\times10^{-2}$ $R^2=0.998$	$(2.20\pm0.20)\times10^{-4}$	167.5 ± 1.00
	303	$[AD]=3.65\times10^{-4}/([SAC]-5.72\times10^{-2})+5.72\times10^{-2}$ $R^2=0.998$	$(3.65\pm0.11)\times10^{-4}$	156.8 ± 0.97
	313	$[AD]=3.15\times10^{-3}/([SAC]-8.05\times10^{-2})+8.05\times10^{-2}$ $R^2=0.992$	$(3.15\pm0.099)\times10^{-3}$	25.66 ± 0.0023

Alhalaweh *et al.*(30), the cocrystal solubility would be expressed by the following Eq. (11)

$$[AD]_{total} = \frac{K_{sp}}{[SAC]_{solid}} + K_{11}K_{sp} \quad (5)$$

This equation predicts that the solubility of AD-SAC cocrystal at the existence of solution complexation will be greater by a constant value (the product of K_{sp} and K_{11}) than the situation when there is no solution complexation (30). For this case of AD-SAC, $K_{11}K_{sp}$ of AD-SAC is not far less than [SAC]. So using Eq. (5) will remarkably underestimate the cocrystal solubility. This thermodynamics for AD-SAC cocrystal is distinctive from the existing cocrystal systems.

Ternary Phase Diagrams (TPDs)

TPDs for the three-component system at different temperatures were constructed using the solubilities of AD in SAC solutions and the solubilities of AD and SAC in pure solvents (Figs. 4, 5, and 6). The concentrations of AD and SAC were converted to the percentage in the system. TPDs can show the total composition of the solid and liquid phases of the cocrystal system, and demonstrate the impact of solvent and temperature on AD-SAC cocrystal formation.

Each TPD can be divided into six regions. For example, regions 1, 2, and 3 shown in Fig. 6b represent that the solution was in equilibrium with the solid phases of AD-SAC cocrystal, AD, and SAC, respectively. In region 4 and 5, cocrystal coexists with AD and SAC, respectively. Region 6 represents an under-saturated solution condition which is bounded by the solubility curves of AD (ab), cocrystal (bc), and SAC (cd). Points a and d are the solubilities of AD and SAC, respectively. Point b and point c are two ternary-phase points. The arc lines between b and c are the cocrystal solubility curve corresponding to the parabolas in Fig. 3.

In each TPD, the cocrystal solubility curve (bc) crosses the 1:1 stoichiometric ratio line (Ae) to create an intersection point (f). This demonstrates the possibility of cocrystallization from a stoichiometric solution in all solvents and all temperatures studied (277–313 K). These cocrystals are congruently saturating systems which have a tendency to form AD-SAC cocrystal in the stable cocrystal region 1 (21).

The temperature has an obvious effect on TPDs and the cocrystallization behaviors in three solvents. The lower the temperature, the shorter the distance (Af) between the triangle vertex and the intersection point. This indicates that lower temperature accelerates the cocrystallization process. At the same time, the under-saturated solution region 6 has the smallest area.

The stable cocrystal region (region 1) in ethyl acetate is distinctly more symmetric than those in ethanol and isopropanol (Fig. 6). This is due to the very similar solubilities of AD and SAC in ethyl acetate. That means that cocrystal regions are symmetrically presented at both left and right sides of the stoichiometric ratio line. It will be easier to isolate the cocrystal from the solvent using stoichiometric ratio of API and coformer. However, in ethanol and isopropanol, significantly higher solubility of AD than SAC makes the cocrystal regions shrink to the left side (Figs. 4 and 5). Although the solubility curve of cocrystal can still intersect with the 1:1 stoichiometric ratio line and the cocrystal can be isolated from the solvent, an excess amount of AD should be used. This may cause the waste of AD and increase the costs for cocrystal production. Meanwhile, the solubility ratio of AD and SAC in ethanol and isopropanol is increased from about 3.5 fold at 277 K to nearly 8 fold at 313 K. Only a small cocrystal region is on the right side at 313 K (Figs. 4d and 5d). More AD in the system is necessary to make cocrystallization occur under this condition. These systems suffer from the risk of crystallizing the single component. Therefore, for AD-SAC cocrystal, these TPDs provide the important information to identify the optimizing crystallization condition, such as a suitable solvent type and temperature. Ethyl acetate can be used as the optimum solvent for AD-SAC cocrystal production, especially at lower temperature.

Thermodynamic Parameters

If 1:1 AD-SAC cocrystal dissolves into its individual components, the solubility of cocrystal ($S_{AD\text{-}SAC}$) equals to the concentration of AD ([AD]) and SAC ([SAC]). Substituting this equivalent relationship into Eq. (4) will give:

$$S_{AD-SAC} = \sqrt{K_{sp}} + K_{11}K_{sp} \quad (6)$$

According to the calculated K_{sp} and K_{11} estimated from AD-SAC cocrystal solubility in different solvents, the solubilities of cocrystal in three solvents at different temperatures are listed in Table I. The solubility of cocrystal is significantly lower than those of AD and SAC, suggesting the greater interaction between AD and SAC than that between each component and the solvent.

For 1:1 AD-SAC cocrystal, the cocrystal reaction between AD and SAC is given by

$$AD_{solid} + SAC_{solid} \rightarrow AD{-}SAC_{solid} \quad (7)$$

Incorporating the balance in solution system shown in Eq. (1), the standard free energy change ($\Delta G°$) is generally approximated by

$$\Delta G = -RT\ln\frac{S_{AD}S_{SAC}}{Ksp} \quad (8)$$

Where S_{AD} and S_{SAC} represent the solubility of pure AD and SAC, respectively.

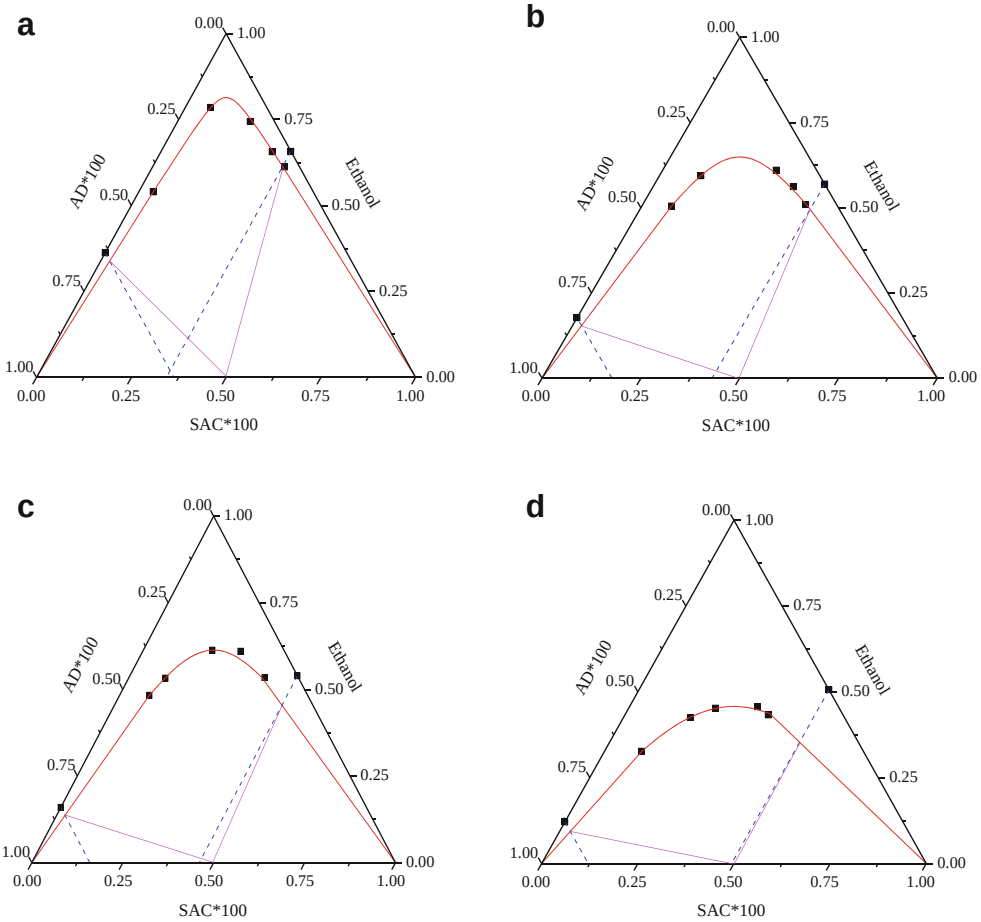

Fig. 4 Ternary phase diagrams of AD-SAC- ethanol system at 277 K (**a**), 293 K (**b**), 303 K (**c**), and 313 K (**d**).

Each set of solubility data in Table I and K_{sp} data in Table II were entered into Eq. (8) to generate the free energy change associated with formation of the cocrystal. The results are listed in Table I. At each temperature, $\Delta G°$ is negative which indicates the formation of cocrystal is spontaneous even at high temperature of 40°C. The absolute amount of $\Delta G°$ gradually decreases with increasing temperature, implying the relative lower ability to form cocrystals at high temperature. However, the free energy changes are similar in three solvents, because of the inexistence of solvent when calculating the $\Delta G°$ for the formation of AD-SAC cocrystal using reaction 7 (22).

Compared to CBZ-NCT system (22), the absolute values of negative $\Delta G°$ of AD-SAC system is much smaller, indicating the more spontaneous process of AD-SAC cocrystal formation. This is also supported by the rapid precipitation of AD-SAC cocrystal in several minutes without solvent and temperature changes (3). However, solvent reduction or solution cooling was indispensable for the formation of CBZ-NCT cocrystal (4,32,33).

Supersaturation

Supersaturation is critical in driving the nucleation of crystal and affecting its growth in solution (34). For the 1:1 AD-SAC cocrystal, supersaturation ratio (S_R) is dependent on the solution composition of the three-component system and can be expressed by (35)

$$S_R = \sqrt{\frac{[\mathrm{AD}][\mathrm{SAC}]}{Ksp}} \tag{9}$$

It's conventional that supersaturation increases with increasing concentrations of AD and SAC in each solvent. At a given AD/SAC ratio, S_Rs in isopropanol and ethyl acetate are comparable but much higher than that in ethanol. For example, at AD/SAC ratio of 0.1:0.1, the supersaturation ratio is 3.77 in ethanol, which is only about half of those in isopropanol and ethyl acetate.

However, it should be noted that supersaturation is an integrated parameter in evaluating the crystal nucleation. The solvent, the concentrations of components and their ratio, as well as temperature should also be taken into consideration when comparing the supersaturation. For example, the supersaturation in ethyl acetate at AD/SAC ratio of 0.05:0.07 was 3.99; lower than the supersaturation value in ethanol at AD/SAC ratio of 0.2:0.1(5.33).

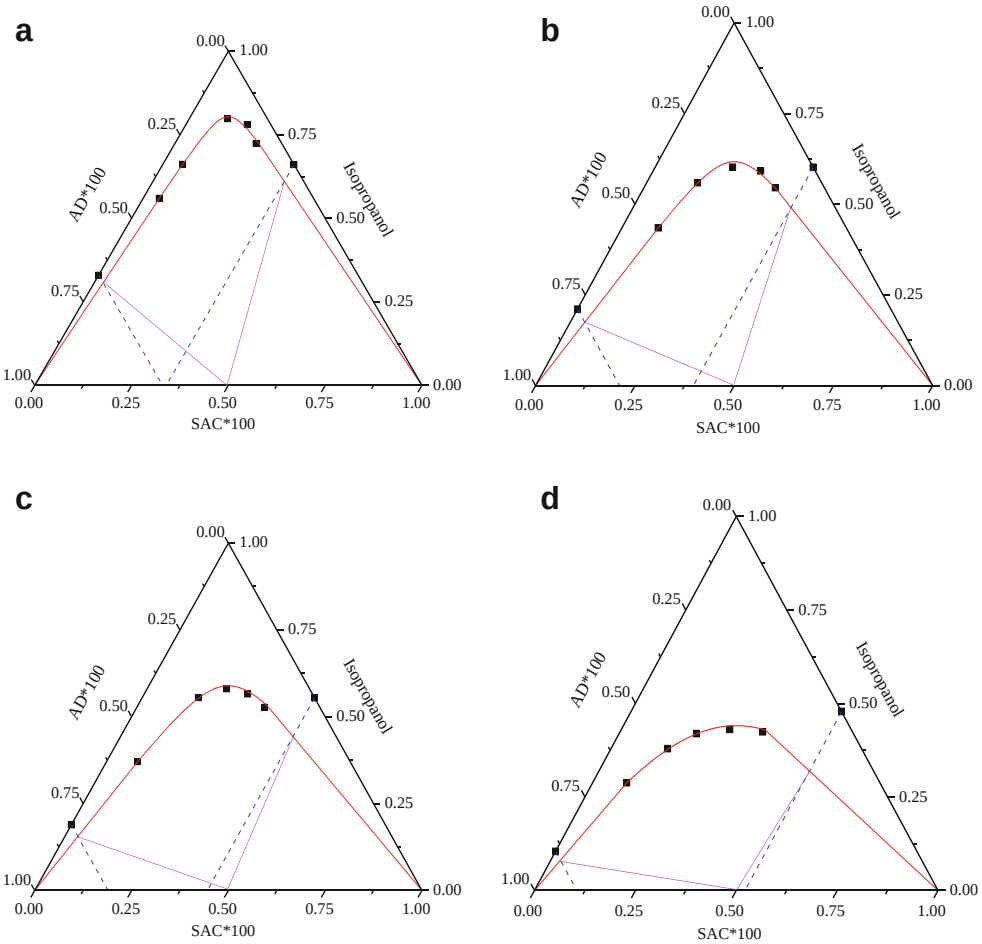

Fig. 5 Ternary phase diagrams of AD-SAC- isopropanol system at 277 K (**a**), 293 K (**b**), 303 K (**c**), and 313 K (**d**).

Nucleation Parameters

AD-SAC system (0.1 mol/L:0.1 mol/L) at 293 K was used as a model to investigate the cocrystallization kinetics in three solvents. The correlation between induction period (τ) and supersaturation ratio (S_R) at a given temperature can be established based on Nielsen theory, which was generally given by (26,36):

$$\log \tau = \frac{B}{T^3 (\log S_R)^2} + A \tag{10}$$

Where A and B are constant. B is given by

$$B = \frac{\beta \gamma^3 \upsilon^2}{(2.303 k_B \mathrm{T})^3 v^2} \tag{11}$$

where k_B is the Boltzmann constant (1.38×10^{-23} J/K), T is the absolute temperature (K), γ is the interfacial energy between the crystal and the aqueous solution (J/m^2), υ is the molar volume of AD-SAC cocrystal (8.46×10^{-28} m^3, calculated by Materials Studio 5.0), v is the mole number (v = 2 for AD-SAC cocrystal), and β is a structural factor ($\beta = 16\pi/3$ for the spherical nucleus and 4 for square nucleus).

For all solvent systems, $\log(\tau)$ and $(\log S_R)^{-2}$ are fitted with linear regression. All the r^2 are greater than 0.99 and this indicates the good linearity. The slope the fitted line in ethanol is significantly lower than those in isopropanol and ethyl acetate. In specificity, the linear relationship between $\log(\tau)$ and $(\log S_R)^{-2}$ in ethanol, and ethyl acetate are $\log(\tau) = 0.4419/(\log S_R)^2 + 1.7727$, $\log(\tau) = 0.8522/(\log S_R)^2 + 0.8818$, and $\log(\tau) = 0.8437/(\log S_R)^2 + 0.8402$, respectively. For isopropanol and ethyl acetate, the slopes and intercepts are comparable and therefore they may have the similar nucleation process.

These regression curves can be used as indicators for predicting the induction period and deciding S_R. For ethanol and ethyl acetate, their regression lines are crossed at $\log S_R = 0.6564$ (or $S_R = 4.533$). Therefore, the comparison of induction period at the same supersaturation ratio or the supersaturation ratio at the same induction period depends on the region of supersaturation. When S_R is lower than 4.533, the induction period in ethanol will be shorter than that in isopropanol and ethyl acetate. To achieve the same induction

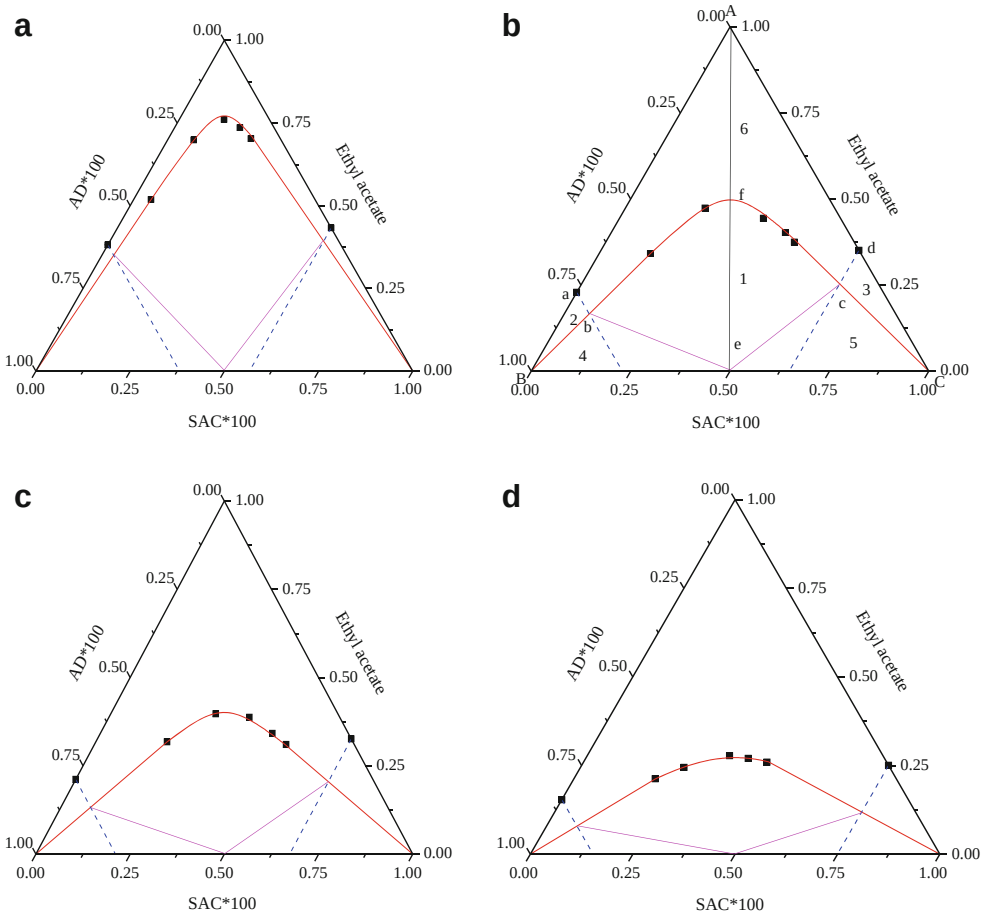

Fig. 6 Ternary phase diagrams of AD-SAC-ethyl acetate system at 277 K (**a**), 293 K (**b**), 303 K (**c**), and 313 K (**d**).

period, higher S_R is required for isopropanol and ethyl acetate systems. However, S_R in isopropanol and ethyl acetate was 60–80% higher than that in ethanol. So the induction period in ethanol was still longer at the same AD/SAC ratio in isopropanol and ethyl acetate, as confirmed by the measured values.

Several parameters of AD-SAC cocrystal, including critical free energy, surface energy, critical nucleus radius, and numbers of the particles in a nucleus, are important to be considered for evaluating the cocrystallization kinetics. However, it is quite difficult to obtain these parameters because of the complex intermolecular solute-solute and solute-solvent forces, and the collisions with the impeller (paddle) and other parts of the reaction containers (37). Although the complexity of the cocrystallization interaction in the solution is still not well understood, the necessity of the proto-cocrystal is a common view. In the beginning, the AD-SAC cocrystal molecules are easily to be dissociated by the forces from diffusion, interfacial effects, hydrodynamics, and collision. However, it is not enough to induce nucleation, even the molecules can stay together for a while. The proto-cocrystal possesses the combined attractive forces between the cocrystal molecules which are strong enough to resist other forces in the solution. At the same time, the proto-cocrystal acts as the nucleation site to allow the subsequent growth in the solution. The generated sufficiently stable nuclei will gradually make the cocrystal grow into crystals of visible size.

At the critical state for the formation of proto-cocrystal, the energy change per unit volume (ΔG_v) is expressed as (38)

$$\Delta G_v = -\frac{k_B T \ln S_R}{\upsilon} \tag{12}$$

Table III Nucleation Parameters of AD-SAC Cocrystal

Solvents	Interfacial tension γ (J/m^2)	Critical radius r (m)	Critical number n*	ΔG$_v$(J/m^3)	Critical free energy ΔG* (J)
Ethanol	7.93E-03	2.50E-09	19	-6.34×10^6	2.08 E-19
Isopropanol	6.12E-03	1.35E-09	13	-9.08×10^6	4.66 E-20
Ethyl acetate	6.10E-03	1.34E-09	12	9.13×10^6	4.57 E-20

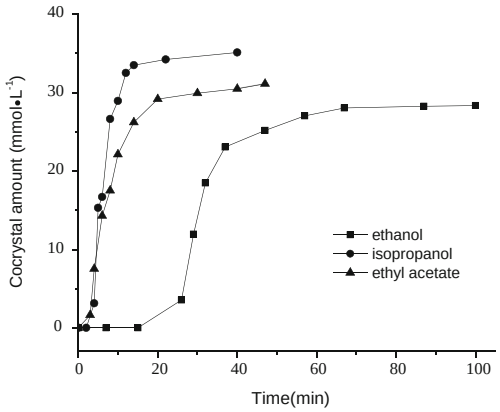

Fig. 7 The cocrystal growth curve at an AD/SAC ratio of 0.1:0.1 (mol/L: mol/L) in ethanol (*black square*), isopropanol (*black circle*), and ethyl acetate (*black triangle*).

The critical nucleus radius (r*) of cocrystal can be calculated by (38)

$$r^* = \frac{2\gamma v}{k_B T \ln S_R} \tag{13}$$

The critical Gibbs free energy barrier for the formation of the critical nucleus in terms of the supersaturation is given as (39,40):

$$\Delta G^* = \frac{16\pi\gamma^3 v^2}{3k_B^2 T^2 (\ln S_R)^2} \tag{14}$$

The numbers of the particles in a critical nucleus (N_m) can be obtained by (40)

$$N_m = \frac{2\beta\gamma^3 v^2}{(k_B T \ln S_R)^3} \tag{15}$$

After transformation of Eq. (11), interfacial energy (γ) can be calculated by

$$\gamma = 2.303 k_B T \sqrt[3]{\frac{Bv^2}{\beta v^2}} \tag{16}$$

These important parameters for cocrystallization nucleation are presented in Table III.

Interfacial energy plays an important role in the initial formation of stable nuclei. Longer induction time will be needed for higher interfacial tension. The clusters must reach a critical nuclei size so as to proceed the crystallization (41). The critical cocrystal nuclei size in ethanol is as twice big as that in the other two solvents and more particles exist in the critical nucleus. It can be inferred that proto-cocrystal in ethanol is easy to be broken apart and more particles are needed to construct the sufficiently stable nuclei. So the free energy barrier in ethanol should be higher, as demonstrated by ΔG* values in Table III. Critical free energy ΔG* works as

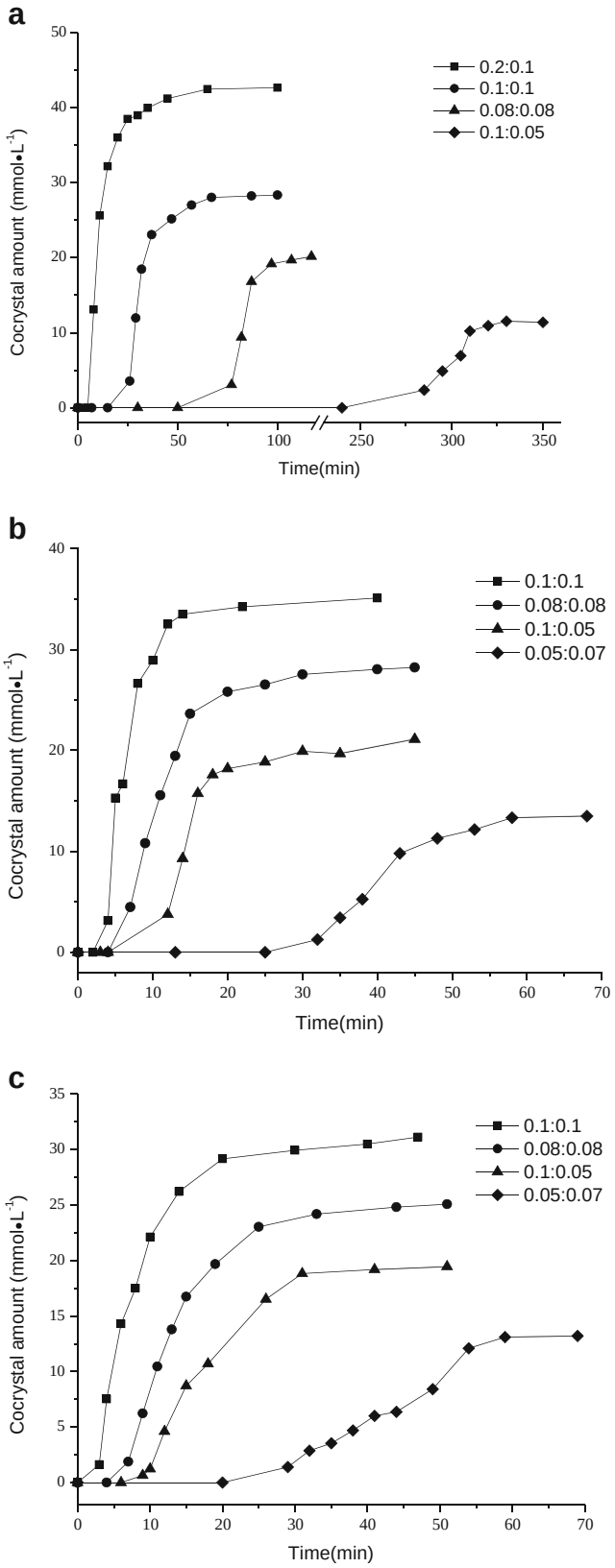

Fig. 8 The cocrystal growth curves at different AD/SAC ratios in ethanol (**a**), isopropanol (**b**) and ethyl acetate (**c**).

an activation energy. This level must be overcome in order for crystallization to continue (41). Thus, use of isopropanol and ethyl acetate as the solvent reduces the energy barrier for nucleation and increases nucleation rate.

Dynamic Cocrystallization

The amounts of the formed solid cocrystals in the three solvents were plotted as a function of time. Figure 7 compares the growth rate of AD:SAC (0.1 mol/L:0.1 mol/L) system in three solvents. Obviously, each growth curve can be divided into three phases: lag phase (induction period), massive increase phase and steady growth phase. The induction period of ethanol system is 15 min, which is about 5 times longer that of isopropanol or ethyl acetate. After their respective induction period, massive growth of cocrystal begins, reflected by the steep slopes in isopropanol and ethyl acetate. However, another 8 min are necessary for this sharp cocrystallization to occur in ethanol. About 10 min later, the cocrystallization in isopropanol and ethyl acetate reaches the relatively steady phase and then slow growth starts. The rapid growth stage in ethanol is also much slower. This is in consistent with the comparative critical free energy (ΔG^*). Using isopropanol and ethyl acetate as the cocrystallization solvent, significantly greater amount of cocrystal can be harvested at the same AD/SAC ratio and inputs. Specifically, the order of cocrystal yield is ethyl acetate > isopropanol > ethanol.

Figure 8 shows the effect of AD/SAC ratios on the growth profiles of cocrystal in three solvents. In each solvent, the induction period increases and the amount of obtained cocrystal decreases with decreasing amount of AD/SAC. At an AD/SAC ratio of 0.1:0.05, the induction period in ethanol is even more than 4 h. The cocrystal amount in 6 h is < 15 mmol/L, which is only about 28% of that at AD/SAC ratio of 0.2:0.1. Although the induction time curtails significantly and the cocrystal yield is improved in isopropanol and ethyl acetate, such trend maintains. This simple but efficient technique achieved a continuous and dynamic measurement of precipitated cocrystal about nucleation and growth rate, as well as the actual amount of cocrystals measured. It will be very conducive to the intuitive investigation and selection of cocrystallization parameters, including composition parameters such as the solvent, API/CCF ratio, the input amount of API and CCF, the process parameters such as temperature and/or cooling rate, stirring speed. All these parameters are complicated but crucial for the scaling-up of cocrystallization process which is still a difficult task at present (8). The scale-up of crystallization process from lab to manufacturing plant is usually challenging (42), which is batch-dependent and can be affected by many factors, such as the change in crystallization rate, stirring and many intricate operational aspects (43). This situation may become more serious due to the more complex nature of cocrystallization (30,31).

CONCLUSIONS

This study investigated the thermodynamic and kinetic profiles of AD-SAC cocrystal in terms of the spontaneous cocrystallization in organic solvents, without the necessity of the change in solvent amount and temperature. AD/SAC system was demonstrated to be a good example for the significance of $K_{sp}K_{11}$ (the product of K_{sp} and K_{11}) to avoid the underestimation of the cocrystal solubility. It provides a good supplement to the present cocrystal research area. This groundwork may be used to guide the scale-up of cocrystallization, including supersaturation, nucleation, crystal growth, and cocrystal yield. The simple, intuitive and efficient technique used in this study may be conducive to the investigation into dynamic cocrystallization and optimization of the cocrystallization parameters. The results of the present study made the subsequent scaling up of AD-SAC cocrystal promising. In future work, some crystallizer parameters are to be covered to achieve the optimized batch product of cocrystal.

ACKNOWLEDGMENTS

This research was supported by the Important National Science & Technology Specific Projects (NO. 2011ZX09201-101-02), The National Natural Science Fund (NO. 81202988) and the Fundamental Research Funds for the Central Universities (Program No. JKP2011006).

REFERENCES

1. Miroshnyk I, Mirza S, Sandler N. Pharmaceutical co-crystals-an opportunity for drug product enhancement. Expert Opin Drug Del. 2009;6(4):333–41.
2. Shayanfar A, Asadpour-Zeynali K, Jouyban A. Solubility and dissolution rate of a carbamazepine–cinnamic acid cocrystal. J Mol Liq. 2013;187:171–6.
3. Gao Y, Zu H, Zhang J. Enhanced dissolution and stability of adefovir dipivoxil by cocrystal formation. J Pharm Pharmacol. 2011;63(4):483–90.
4. Trask AV, Motherwell WD, Jones W. Physical stability enhancement of theophylline via cocrystallization. Int J Pharm. 2006;320(1):114–23.
5. Karki S, Friščić T, Fábián L, Laity PR, Day GM, Jones W. Improving mechanical properties of crystalline solids by cocrystal formation: new compressible forms of paracetamol. Adv Mater. 2009;21(38–9):3905–9.
6. Jung MS, Kim JS, Kim MS, Alhalaweh A, Cho W, Hwang SJ, *et al.* Bioavailability of indomethacin-saccharin cocrystals. J Pharm Pharmacol. 2010;62(11):1560–8.
7. Chow SF, Chen M, Shi L, Chow AH, Sun CC. Simultaneously improving the mechanical properties, dissolution performance, and hygroscopicity of ibuprofen and flurbiprofen by cocrystallization with nicotinamide. Pharm Res. 2012;29(7):1854–65.
8. Ainouz A, Authelin JR, Billot P, Lieberman H. Modeling and prediction of cocrystal phase diagrams. Int J Pharm. 2009;374(1):82–9.

9. Schultheiss N, Newman A. Pharmaceutical cocrystals and their physicochemical properties. Cryst Growth Des. 2009;9(6):2950–67.
10. Padrela L, Rodrigues MA, Velaga SP, Fernandes AC, Matos HA, De Azevedo EG. Screening for pharmaceutical cocrystals using the supercritical fluid enhanced atomization process. J Supercrit Fluid. 2010;53(1):156–64.
11. Nehm SJ, Rodríguez-Spong B, Rodriguez-Hornedo N. Phase solubility diagrams of cocrystals are explained by solubility product and solution complexation. Cryst Growth Des. 2006;6(2):592–600.
12. Chiarella RA, Davey RJ, Peterson ML. Making co-crystals the utility of the ternary phase diagram. Cryst Growth Des. 2007;7(7):1223–6.
13. Gagniere E, Mangin D, Puel F, Bebon C, Klein JP, Monnier O, *et al.* Cocrystal formation in solution: in situ solute concentration monitoring of the two components and kinetic pathways. Cryst Growth Des. 2009;9(8):3376–83.
14. Derdour L, Fevotte G, Puel F, Carvin P. Real-time evaluation of the concentration of impurities during organic solution crystallization. Powder Technol. 2003;129(1):1–7.
15. Gagniere E, Mangin D, Puel F, Rivoire A, Monnier O, Garcia E, *et al.* Formation of co-crystals: kinetic and thermodynamic aspects. J Cryst Growth. 2009;311(9):2689–95.
16. Starrett JEJ, Tortolani DR, Russell J, Hitchcock MJ, Whiterock V, Martin JC, *et al.* Synthesis, oral bioavailability determination, and in vitro evaluation of prodrugs of the antiviral agent 9-[2-(phosphonomethoxy) ethyl] adenine (PMEA). J Med Chem. 1994;37(12):1857–64.
17. Gao Y, Gao J, Liu Z, Kan H, Zu H, Sun W, *et al.* Coformer selection based on degradation pathway of drugs: a case study of adefovir dipivoxil-saccharin and adefovir dipivoxil-nicotinamide cocrystals. Int J Pharm. 2012;438(1–2):327–35.
18. Hickey MB, Peterson ML, Scoppettuolo LA, Morrisette SL, Vetter A, Guzmán H, *et al.* Performance comparison of a co-crystal of carbamazepine with marketed product. Eur J Pharm Biopharm. 2007;67(1):112–9.
19. Nokhodchi A, Bolourtchian N, Dinarvand R. Crystal modification of phenytoin using different solvents and crystallization conditions. Int J Pharm. 2003;250(1):85–97.
20. Zhang J, Zu H, Gao Y. Formation thermodynamics of adefovir dipivoxil-saccharin co-crystals. Acta Phys-Chim Sin. 2011;27(3):547–52.
21. Good DJ, Rodríguez-Hornedo N. Solubility advantage of pharmaceutical cocrystals. Cryst Growth Des. 2009;9(5):2252–64.
22. Schartman RR. On the thermodynamics of cocrystal formation. Int J Pharm. 2009;365(1):77–80.
23. Crosio MP, Jullien M. Fluorescence study of precrystallization of ribonuclease A: effect of salts. J Cryst Growth. 1992;122(1):66–70.
24. Michinomae M, Mochizuki M, Ataka M. Electron microscopic studies on the initial process of lysozyme crystal growth. J Cryst Growth. 1999;197(1):257–62.
25. Kozlovskii MI, Wakita H, Masuda I. Analyses of precipitation processes of bis (dimethylglyoximato) Ni (II) and related complexes. J Cryst Growth. 1983;61(2):377–82.
26. Kuldipkumar A, Kwon GS, Zhang GG. Determining the growth mechanism of tolazamide by induction time measurement. Cryst Growth Des. 2007;7(2):234–42.
27. Van der Leeden MC, Kashchiev D, Van Rosmalen GM. Precipitation of barium sulfate: Induction time and the effect of an additive on nucleation and growth. J Colloid Interf Sci. 1992;152(2):338–50.
28. Söhnel O, Mullin JW. A method for the determination of precipitation induction periods. J Cryst Growth. 1978;44(4):377–82.
29. Childs SL, Rodríguez-Hornedo N, Reddy LS, Jayasankar A, Maheshwari C, McCausland L, *et al.* Screening strategies based on solubility and solution composition generate pharmaceutically acceptable cocrystals of carbamazepine. CrystEngComm. 2008;10(7):856–64.
30. Alhalaweh A, Sokolowski A, Rodríguez-Hornedo N, Velaga SP. Solubility behavior and solution chemistry of indomethacin cocrystals in organic solvents. Cryst Growth Des. 2011;11(9):3923–9.
31. Higuchi T, Connors KA. Phase-solubility techniques. Adv Anal Chem Instrum. 1965;4(2):117–212.
32. Alhalaweh A, Velaga SP. Formation of cocrystals from stoichiometric solutions of incongruently saturating systems by spray drying. Cryst Growth Des. 2010;10(8):3302–5.
33. Rahman Z, Agarabi C, Zidan AS, Khan SR, Khan MA. Physicomechanical and stability evaluation of carbamazepine cocrystal with nicotinamide. AAPS PharmSciTech. 2011;12(2):693–704.
34. Lee KC, Kim KJ. Effect of supersaturation and thermodynamics on co-crystal formation. Chem Eng Technol. 2011;34(4):619–23.
35. Rodríguez-Hornedo N, Nehm SJ, Seefeldt KF, Pagán-Torres Y, Falkiewicz CJ. Reaction crystallization of pharmaceutical molecular complexes. Mol Pharmaceut. 2006;3(3):362–7.
36. Yi WT, Yan CY, Ma PH. Crystallization kinetics of Li_2CO_3 from $LiHCO_3$ solutions. J Cryst Growth. 2010;312(16):2345–50.
37. Tung HH, Paul EL, Midler M, McCauley JA. Crystallization of organic compounds: an industrial perspective. New Jersey: Wiley-AIChE; 2009.
38. Selvaraju K, Valluvan R, Kumararaman S. Experimental determination of metastable zone width, induction period, interfacial energy and growth of nonlinear optical Hippuric acid single crystal. Mater Lett. 2006;60(12):1549–53.
39. Liu X, Wang Z, Duan A, Zhang G, Wang X, Sun Z, *et al.* Measurement of l-arginine trifluoroacetate crystal nucleation kinetics. J Cryst Growth. 2008;310(10):2590–2.
40. Nielsen AE, Sarig S. Homogeneous nucleation of droplets and interfacial tension in the liquid system methanol-water-tribromomethane. J Cryst Growth. 1971;8(1):1–7.
41. Storey RA, Ymén I. Solid state characterization of pharmaceuticals. Chichester: Wiley-Blackwell; 2011.
42. Desikan S, Anderson SR, Meenan PA, Toma PH. Crystallization challenges in drug development: scale-up from laboratory to pilot plant and beyond. Curr Opin Drug Discov Dev. 2000;3(6):723–33.
43. Beckmann W. Crystallization- basic concepts and industrial applications. Weinheim: Wiley-VCH Verlag GmbH & Co. KGaA; 2013.